Available online at www.sciencedirect.com
SCIENCE DIRECT®
Biochemical and Biophysical Research Communications 310 (2003) 19–27
BBRC
www.elsevier.com/locate/ybbrc

Deacylation activity of cephalosporin acylase to cephalosporin C is improved by changing the side-chain conformations of active-site residues

Bora Oh,[a] Myungsook Kim,[a] Jongchul Yoon,[a] Kyungwha Chung,[b] Yongchul Shin,[b] Dongsoon Lee,[c,d] and Youngsoo Kim[a,d,*]

[a] *Division of Molecular Genomic Medicine, College of Medicine, Seoul National University, Yongon-Dong, Seoul 110-799, Republic of Korea*
[b] *Amicogen Company, 694-4, Jinsung, Jinju 660-852, Republic of Korea*
[c] *Department of Clinical Pathology, College of Medicine, Seoul National University, Yongon-Dong, Seoul 110-799, Republic of Korea*
[d] *Cancer Research Institute, College of Medicine, Seoul National University, Yongon-Dong, Seoul 110-799, Republic of Korea*

Received 2 August 2003

Abstract

Semisynthetic cephalosporins are primarily synthesized from 7-aminocephalosporanic acid (7-ACA), mainly by environmentally toxic chemical deacylation of cephalosporin C (CPC). Thus, the enzymatic conversion of CPC to 7-ACA by cephalosporin acylase (CA) would be very interesting. However, CAs use glutaryl-7-ACA (GL-7-ACA) as a primary substrate and the enzymes have low turnover rates for CPC. The active-site residues of a CA were mutagenized to various residues to increase the deacylation activity of CPC, based on the active-site conformation of the CA structure. The aim was to generate sterically favored conformation of the active-site to accommodate the D-α-aminoadipyl moiety of CPC, the side-chain moiety that corresponds to the glutaryl moiety of GL-7-ACA. A triple mutant of the CA, Q50βM/Y149αK/F177βG, showed the greatest improvement of deacylation activity to CPC up to 790% of the wild-type. Our current study is an efficient method for improving the deacylation activity to CPC by employing the structure-based repetitive saturation mutagenesis.

Keywords: Cephalosporin acylase; Penicillin acylase; 7-Aminocephalosporanic acid; Glutaryl-7-aminocephalosporanic acid; Protein engineering; Substrate specificity

Semi-synthetic cephalosporins are the most widely used antibiotics. Semi-synthetic cephalosporins are primarily synthesized from 7-aminocephalosporanic acid (7-ACA), a starting compound that can be obtained by the deacylation of cephalosporin C (CPC). In contrast to the enzymatic production of 6-aminopenicillanic acid (6-APA) by penicillin G acylase (PGA) for synthesizing semi-synthetic penicillins [1], the industrial production of 7-ACA is largely carried out by chemical methods using toxic compounds, such as iminoether, nitrosyl chloride, and methanol [2].

Four thousand tons of 7-ACA is annually produced from CPC by the pharmaceutical industry, but the majority of 7-ACA is manufactured by toxic chemical deacylation (Amicogen Company, Korea, personal communication). Therefore, a conversion of CPC to 7-ACA by enzymatic reaction has been of great interest. However, cephalosporin acylases (CAs) use glutaryl-7-ACA (GL-7-ACA) as a primary substrate and the enzyme has low turnover rates for CPC [3,4]. Unsuccessful attempts to obtain a direct enzymatic transformation of CPC into 7-ACA by a single CA have led to the development of an inefficient 2-enzyme process using CA and D-amino acid oxidase (DAAO) [5].

All CAs in the five classes have different substrate specificities to GL-7-ACA and CPC, and their activities to CPC vary from 0% to 4.0% relative to GL-7ACA (Table 1). Out of the five different classes of CAs, the class I and III CAs have the highest activity to CPC

* Corresponding author. Fax: +82-2-741-7947.
E-mail address: biolab@snu.ac.kr (Y. Kim).

0006-291X/$ - see front matter © 2003 Elsevier Inc. All rights reserved.
doi:10.1016/j.bbrc.2003.08.110

Table 1
Substrate specificity profiles of cephalosporin acylases

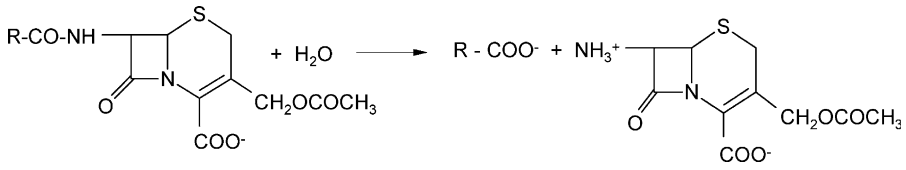

Substrate	R	Relative enzyme activity[a]				
		P130[b] (class I)	A14[c] (class II)	N176[c] (class III)	acyI[d] (class IV)	J1[c] (class V)
GL-7-ACA	HOOC-$(CH_2)_{3-}$ (glutaryl)	100	100	100	100	100
CPC	HOOC-CH(NH_2)-$(CH_2)_{3-}$ (D-α-aminoadipyl)	2.3	<0.009	4	0	<0.009

[a] The deacylation reaction of cephalosporins is shown above; the different side chains indicated by R. Relative enzyme activity was expressed as a percentage compared to the activity for GL-7-ACA for each enzyme. P130, A14, N176, acyI, and J1 stand for the cephalosporin acylases from *Pseudomonas* sp. 130, A14, N176, SE83, and *Bacillus laterosporus* J1, respectively.
[b,c,d] Reaction conditions and data are described by Aramori et al. (1992), Matsuda et al. (1987), and Li et al. (1999), respectively [3,4,8].

(Table 1) [3,4,6,7]. This low activity to CPC has hampered the application of CAs to the industrial production of 7-ACA. Intensive site-directed mutagenesis was carried out on a class III CA (a CA from *Pseudomonas diminuta* (N176)) to improve the activity to CPC, which was not successful [6,7].

The gene structure of the open-reading frame of CAs consists of a signal peptide followed by an α-subunit, a spacer sequence, and a β-subunit. The CAs genes are translated into an inactive single precursor polypeptide that is post-translationally modified into a mature enzyme with one α-subunit and one β-subunit [8]. All known CAs use either Ser or Thr as a key nucleophile to carry out both auto-proteolysis and enzymatic deacylation. The precursor polypeptide of CAs is auto-proteolytically activated through a two-step auto-catalytic process upon folding. The first step is an intramolecular cleavage of the precursor at the start of the β-subunit, resulting in an α-subunit, a spacer peptide attached to the C-terminus of the α-subunit, and a β-subunit. The second step is an intermolecular event, which may be mediated by the newly generated N-terminal Ser or Thr of the β-subunit by intramolecular cleavage. The second event results in further cleavage at the second scissile bond and this finally releases the spacer peptide [8–10].

The absence of a three-dimensional structure for CAs has been a handicap for the progress of protein engineering, but the structure of a class I CA from *P. diminuta* (CAD) was recently determined at 2.0 Å resolution (Table 1) [11,12]. In addition, two binary structures in complex with GL-7-ACA (the most favored substrate of all five class CAs) and glutarate (side-chain of GL-7-ACA, which determines substrate specificity in CA) were determined at 2.6 and 2.5 Å resolutions, respectively [13]. These three structures revealed the active-site conformation as well as detailed interactions of GL-7-ACA with residues in the side-chain pocket of the active-site.

In the current report, the active-site residues of CAD were mutagenized by saturation site-directed mutagenesis to increase the deacylation activity to CPC. The residues for mutations were guided by the ligand bound structures of CAD [13]. The aim of the mutations was to generate the sterically favored conformation of the active-site to accommodate the D-α-aminoadipyl moiety of CPC, the side-chain moiety that corresponds to the glutaryl moiety of GL-7-ACA (Table 1).

Materials and methods

Site-directed mutagenesis of CAD. Mutants of CAD were constructed by site-directed mutagenesis using a polymerase chain reaction, as previously described [14]. PCR primers were synthesized so that the three bases for a target residue could have as many kinds of variants (4 different bases at each base position) as possible from a PCR (named saturated site-directed mutagenesis in this paper). The right sized PCR fragment DNAs were ligated into the pET24d(+) vector. The mutant CAD gene on the pET24d(+) plasmid was transformed into an *Escherichia coli* DH5α host cell for further subcloning. The mutant CAD gene was subcloned into *E. coli* BL21(DE3) using the over-expression vector pET24d(+) for the protein expression. All of the DNA manipulations were performed according to standard techniques [15]. All of the mutant genes were sequenced using an automatic DNA sequencer (Perkin–Elmer, USA) to confirm whether or not the targeted mutations were correctly mutated and that no other changes were incorporated.

Expression of mutant CAD protein. The pET24d(+) plasmid bearing mutant CAD was transformed into an *E. coli* BL21(DE3) host cell for the protein over-expression. The *E. coli* BL21(DE3) cells, carrying the pET24d(+) plasmid in a LB medium, were cultured at 37 °C, 250 rpm with 30 μg/ml kanamycin until the O.D. at 600 nm reached 0.6, and then 0.5 mM IPTG was added to the culture at 21 °C for 12 h for protein production. Other details of the overexpression using the pET24d(+) were observed, as described in the Novagen expression system manual (Novagen, USA).

Purification of CAD protein. Purification of the CAD mutants was carried out as previously described [14]. A crude cell extract was prepared by sonication and centrifuged at 12,000*g* for 20 min. The resultant supernatant that was obtained from the centrifugation was concentrated by ammonium sulfate precipitation at 35–50%

saturation. The protein solution was subjected to phenyl Sepharose column chromatography (Pharmacia Biotech, Sweden), which was pre-equilibrated with an equilibration buffer consisting of 30% ammonium sulfate, 1 mM EDTA, 1 mM β-mercaptoethanol (βME), and 50 mM sodium phosphate, pH 7.2. The CAD protein was eluted with a linear gradient of 35–0% ammonium sulfate that was saturated in the equilibration buffer. The eluted protein was concentrated by ultrafiltration and further purified by Sephacryl S-200 gel filtration chromatography (Pharmacia Biotech, Sweden) in case of impurity.

Assay of deacylation activity for mutant CAD. The activity assay for the wild type and mutant CAD was based on the colorimetric measurement [16] of 7-ACA that was released from the substrate GL-7ACA or CPC. Five μl of the enzyme solution (about 10 μg of CAD protein) reacted generally for 1 min in 500 μl of a substrate solution consisting of 1% (w/v) GL-7-ACA, 200 mM sodium phosphate, pH 7.0, 1 mM EDTA, and 1 mM βME. The incubation time for the deacylation reaction for mutant enzymes varied, depending on the reaction speed. The reaction mixture, 40 μl, was transferred into 500 μl of the stop solution (a mixture of acetic acid and 0.25 M NaOH in a 2:1 ratio) and subsequently centrifuged at 12,000 rpm for 10 min. The supernatant was mixed with 35 μl of 5% (w/v) *p*-dimethylaminobenzaldehyde (DAB) in methanol and incubated for 5 min at room temperature. The absorbance was measured at 415 nm wavelength. The protein concentration for the assay was pre-determined by a Bradford assay (Sigma, USA) using bovine serum albumin (BSA) as a standard reagent.

Results and discussion

Interactions between active-site residues and substrates [13]

The structures of the two CAD binary complexes suggested that the most extensive interactions between the protein and a substrate, GL-7-ACA, took place in the glutaryl moiety (the side-chain of GL-7-ACA [13]). Three residues in the side-chain pocket (Arg57β, Tyr149α, and Tyr33β) made tight hydrogen bonds with this critical part of the substrate (Fig. 1A). Gln50β in the side-chain pocket makes no direct hydrogen bonds with the glutaryl moiety of GL-7-ACA, but it may still play a significant role in the substrate binding since its side-chain atoms, OE1 and NE2, and make hydrogen bonds with the side-chain NH1 of the critical Arg57β and the OH of Tyr149α, respectively. These two hydrogen bonds may guide the side-chains of Arg57β and Tyr149α to the proper positions for catalysis.

In addition to the hydrogen bonds of the carboxylate group, four carbon atoms of the glutaryl moiety are stabilized by hydrophobic interactions with neighboring hydrophobic residues. Atoms C15, C17, C5, and C9 of the glutarate moiety are engaged in hydrophobic interactions with atoms CD2 of Leu24β, CD2 of Leu24β, CB of Val70β, and CE2 of Phe177β, respectively. The binding mode of the glutaryl moiety of GL-7-ACA (Fig. 1A) is such that every atom of the carboxylate group, except the C11 carbon atom, interacts with seven active-site residues (Leu24β, Tyr33β, Gln50β, Arg57β, Val70β, Phe177β, and Tyr149α) by either the hydrogen bond or hydrophobic interactions. Most importantly, it was suggested that the hydrophilic and hydrophobic interactions, between the side-chain of the substrate and its binding pocket, are the dominating factors in recognizing the substrate in CA. The precise individual interactions of GL-7-ACA with these 10 residues in the active–site (Fig. 1A) determine the substrate specificity of CA, which makes GL-7-ACA the most favored substrate. In contrast, the side-chain of CPC dramatically reduces activity in all CAs, even though all of the other parts of both substrates are the same.

Mutagenesis of 10 active-site residues interacting with GL-7-ACA

The conformation of the residues in the active-site of CAD was elucidated in detail (Fig. 1A) [13]. In addition, a model of the D-α-aminoadipyl moiety (the side-chain moiety) of CPC that was overlaid onto the refined structure of GL-7-ACA in complex with CAD was built to investigate the differences that cause the dramatic activity change between the glutaryl (side-chain of GL-7-ACA) and D-α-aminoadipyl moieties (side-chain of CPC) (Fig. 1B) [13]. This model showed that the carboxyl and amino groups of the D-α-aminoadipyl moiety in CPC would collide with active-site residues that form the side-chain pocket, such as R57β, Y33β, and Y149α. Based on the GL-7-ACA bound CAD and the model structure of CPC bound CAD, the direction of the protein engineering to improve the deacylation activity to CPC was designed so that it would provide the active-site with appropriate room to accommodate the extra carbon atom and amino group in the D-α-aminoadipyl moiety of CPC.

In order to confirm the effect of the side-chain conformation on catalytic activity, the 10 residues that were involved in the substrate binding (Fig. 1A) were mutagenized to different amino acids. Their effects for catalysis, with regard to GL-7-ACA and CPC, were then determined by comparing the deacylation activity of the mutant CADs to that of the wild-type. Table 2 shows the deacylation activities of mutant CADs in regard to GL-7-ACA and CPC. All of the mutations for the 10 active-site residues decrease deacylation activity in regard to GL-7-ACA. This was predictable because the substrate, GL-7-ACA, made very precise interactions with the active-site residues (Fig. 1A). On the other hand, two mutants (Y33βS and Q50βM; the mutation of Tyr33β to Ser is named Y33βS) in the side-chain pocket showed improved CPC activity, which might be due to the favorable accommodation of the α-aminoadipyl moiety of CPC into the active-site of the mutants.

Analysis of the mutated residues with regard to deacylation activity

The most dramatic effect was obtained from the S1β mutation because S1β is a catalytic nucleophile that will

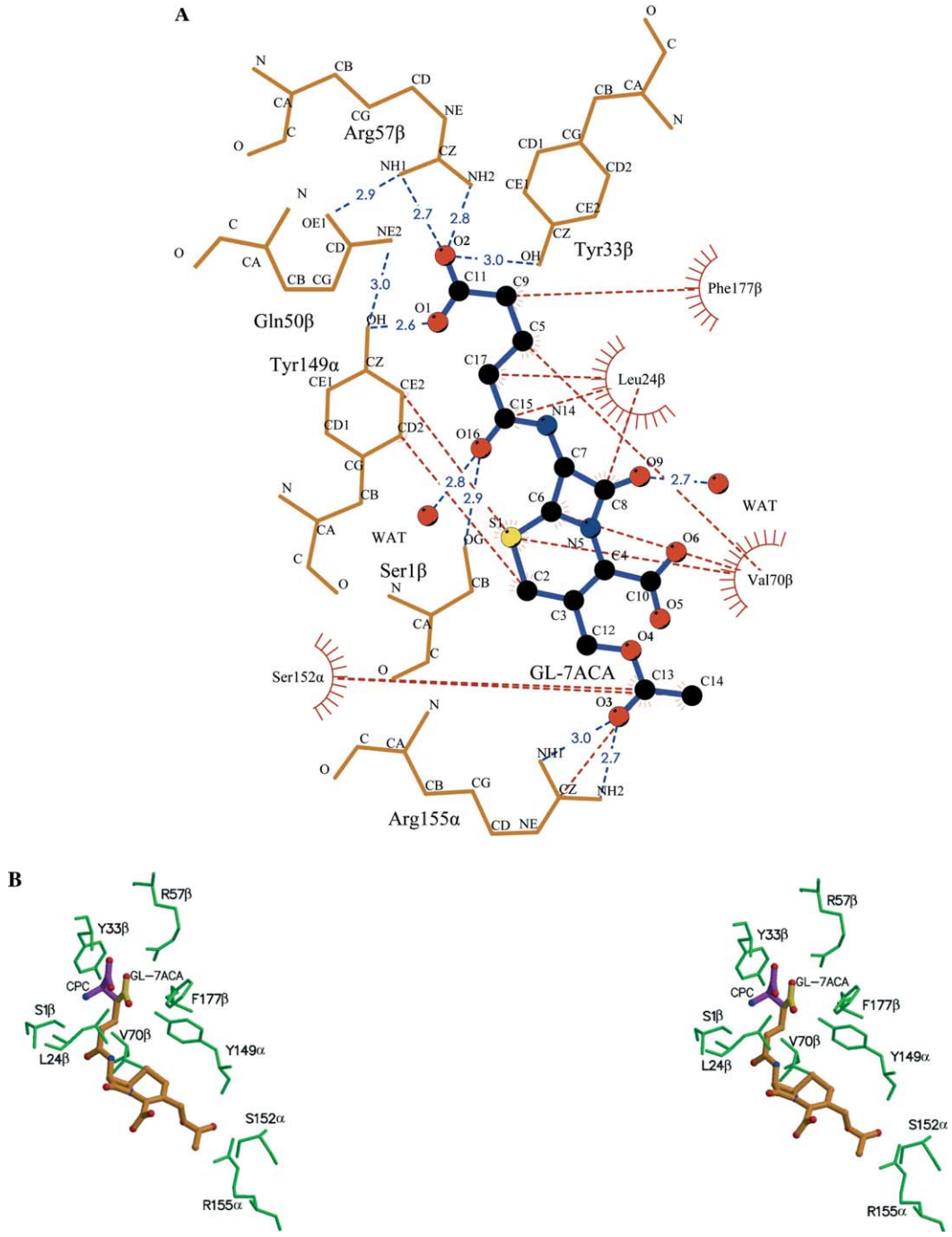

Fig. 1. Binding mode of GL-7-ACA and CPC to active-site of CAD. (A) Detailed interactions between GL-7-ACA and the residues of the active site [13]. The residues that make hydrogen bonds are in yellow stick models in the LIGPLOT [19]. The residues that make hydrophobic interactions are in red, sunny-side circles. Only the distances below 3.4 Å are indicated for hydrogen bonds (blue, dashed lines). Hydrophobic interactions (red, dashed lines) are indicated for distances below 3.9 Å. The ligands are in ball-and-stick models. The carbon-to-nitrogen contacts are not depicted. (B) A model of cephalosporin C overlaid onto the refined GL-7-ACA structure with the nine interacting residues in the active site [13]. GL-7-ACA is shown in orange, except the carboxylate group in the side-chain binding pocket, which is in yellow. All of the CPC atoms are modeled after the refined structure of GL-7-ACA, identical to that shown in orange. However, there is one additional carbon atom. Also, the amino group of the D-α-aminoadipyl moiety, compared to the glutaryl moiety of the GL-7-ACA, is extended to generate the D-α-aminoadipyl moiety (shown in purple). The carboxyl and amino groups of the D-α-aminoadipyl moiety (purple region) crash into the residues of the side-chain binding pocket (Arg57β, Tyr33β, and Tyr149α) when they are rotated by torsional angles.

lose its catalytic capability once it is mutated to a residue. In general, all of the mutations in the seven residues, except S152α and R155α, showed lethal effects for the deacylation of GL-7-ACA, even though the activities decreased in a different fashion according to the residue type (Table 2).

Table 2
Deacylation activity of the active-site residues interacting with substrate with regard to GL-7ACA and CPC

Residue for mutation[a]	Mutated to	GL-7-ACA activity[b] (%)	CPC activity[b] (%)
S1β	Ala	None	None
	Cys	None	None
L24β	Arg	None	87.7
	Gly	27	None
	Trp	11.3	98.8
	Lys	1.1	None
	Phe	None	25.9
Y33β	Phe	65.4	None
	Ile	9.3	90
	Ser	None	120
Q50β	Thr	72.5	70
	Tyr	15.7	None
	Arg	2.1	None
	Leu	9.9	None
	Met	7.5	**180**
R57β	Lys	0.3	None
	Cys	None	None
	Ser	None	None
	Ile	None	None
V70β	Ser	28.8	None
	Gly	None	32.1
F177β	His	17.6	None
	Thr	4.3	None
	Pro	None	None
Y149α	Asn	30.8	48
	Cys	16.4	24
	Arg	13.6	None
	Leu	6.3	48
	Pro	1.1	None
	Gly	0.7	None
S152α	His	63.7	11.9
	Thr	81.4	34.7
	Asn	78	24.8
	Pro	76.2	60.4
	Gly	75.4	38.6
R155α	Gly	88	Not measured
Wild-type		100	100

[a] Template for mutation is wild-type.
[b] GL-7-ACA and CPC activities are compared to the wild-type and less than 0.1% of the deacylation activity is noted as "none".

The R57β and Y33β residues, which are involved in direct hydrogen bonds with the glutaryl moiety of GL-7-ACA, have greater effects on the enzyme activity to GL-7-ACA. Once the R57β and Y33β residues are mutagenized to disrupt the hydrogen bonding patterns, the deacylation activity of the CA mutants is virtually lost. The Y149α mutations are less effective on deacylation than the R57β and Y33β mutations. A less critical effect is also observed in the Q50β mutants because they are involved in the substrate interaction via the indirect hydrogen bond with neighboring residues. The Q50β mutation to other residues might be more tolerable than the three residues (R57β, Y33β, and Y149α) that directly interact with the carboxyl group of glutaryl moiety.

The L24β and V70β mutations that are involved in the hydrophobic interaction with the backbone carbons of GL-7-ACA also had decreased deacylation activity in regard to GL-7-ACA (Table 2). F177β, which is involved in the hydrophobic interaction with the glutaryl side-chain, was mutagenized to several amino acids. Interestingly, the F177β mutants showed highly critical effects on enzymatic activity (Table 2). Since F177β does not make a direct hydrogen bond with the substrate, but instead reveals dramatic effects for mutations, it is conceivable that F177β could be a critical residue that is involved in maintaining the conformation of the active-site. The mutations of the S152α and R155α residues, which are involved in hydrophobic interactions with the

acetoxymethyl chain [13] that is attached to the six-member ring of the two fused β-lactam ring (Table 1) in GL-7-ACA, have no noticeable effects on deacylation activity (Table 2).

In order to understand the mutation effects of the 10 active-site residues on the deacylation of CPC, their deacylation activities were determined (Table 2). Surprisingly, two mutants, Y33βS and Q50βM, showed 120% and 180% of the deacylation activity of the wild-type, respectively. The deacylation activities to GL-7-ACA for Y33βS and Q50βM amounted to 0% and 7.5% relative to the wild-type, respectively. Increasing the deacylation activity to CPC in the two mutants (120% and 180% of wild-type) resulted in a decrease of the deacylation activity to GL-7-ACA (0% and 7.5% of wild-type), which is fairly predictable in view of the close interactions between GL-7-ACA and the active-site residues.

Deacylation activity to CPC for double- and triple-mutated cephalosporin acylases

To improve the deacylation activity to CPC, Q50βM provided a starting point for protein engineering. We added a second mutation to Q50βM to further improve the deacylation activity to CPC. While rotating the modeled α-aminoadipyl moiety (Fig. 1B) in torsion angles, it collided with the Y33β, Y149α, and F58β residues that were placed in that region. In order to generate space to accommodate the D-α-aminoadipyl moiety in the region, the Y33β, Y149α, and F58 residues were mutagenized by saturation mutagenesis to various amino acids with less side-chain volumes. Nine mutants from Y33β, two mutants from Y149α, and nine mutants from F58β were screened. The deacylation activities of those double mutants to CPC were measured (Table 3). Measurements of the deacylation activities to GL-7-ACA for the double mutants were not meaningful because adding the second mutation to Q50M resulted in nearly 0% of the deacylation activity to GL-7-ACA. Apparently, about half of the mutants from the single mutation showed nearly 0% of the deacylation activity to GL-7-ACA (Table 2). Thus, the deacylation activities to GL-7-ACA for triple mutants were also not measured.

All of the double mutants, except Q50βM/Y33βS and Q50βM/Y33βG, showed higher deacylation activities to CPC than the wild-type. Q50βM/Y149αK, Q50βM/Y33βD, and Q50βM/F58βG from the double mutation showed the greatest improvements for the deacylation activity in regard to CPC, to 600%, 450%, and 290% of the wild-type, respectively (Table 3). When these three mutations were visualized by replacing the wild-type with the mutants in the model structure (Fig. 2), it would appear that the three mutants (Q50βM/Y149αK, Q50βM/Y33βD, and Q50βM/F58βG) could generate more space to accommodate the modeled D-α-aminoadipyl moiety of CPC by their lower side-chain volumes (figures not shown). Double mutants of Y33β showed a wide range of deacylation activity to CPC, from 60% to 450% (activity varied more than 7-fold), depending on which of the side-chains were incorporated into the residue.

Table 3
The effect of a second mutation for the mutant Q50βM on deacylation activity with regard to CPC

Residue for mutation[a]	Mutated to	CPC activity[b] (%)
Y33β	Thr	109
	Val	135
	Asn	350
	Asp	**450**
	Ser	60
	Gly	70
	Leu	202
	Pro	99
	His	101
Y149α	Phe	157
	Lys	**600**
F58β	Ser	260
	Asp	130
	Ala	180
	Leu	120
	Thr	230
	Ile	150
	His	160
	Pro	240
	Gly	**290**
Wild-type	Wild	100

[a] Template for mutation is Q50βM.
[b] Legend is the same as in Table 2.

A third mutation on the DNA template of Q50βM/Y149αK was carried out for three residues (F177β, Y33β, and M145α). Modeling of the mutant Q50βM/Y149αK in active-site suggested that those three mutations would be generating better accommodation of the D-α-aminoadipyl side-chain of CPC (data not shown). Mutations for the three residues resulted in higher deacylation activity to CPC when compared to the Q50βM/Y149αK template. The triple mutants, Q50βM/Y149αK/F177βG, Q50βM/Y149αK/Y33βS, and Q50βM/Y149αK/M145αL, showed 787%, 568%, and 704% of the deacylation activities to CPC, respectively, compared to the wild-type. The triple mutant, Q50βM/Y149αK/F177βG, increased its deacylation activity, highest among the three triple mutants by 33% relative to the template of the double mutant Q50βM/Y149αK. This series of mutation experiments could optimize the side-chain conformation of the active-site residues to favorably accommodate the D-α-aminoadipyl moiety of CPC into the side-chain binding pocket so as to maximally increase the deacylation activity to CPC.

It seems that the torsional movements of the side-chains of the active-site residues greatly affected the deacylation activity of GL-7-ACA or CPC. The

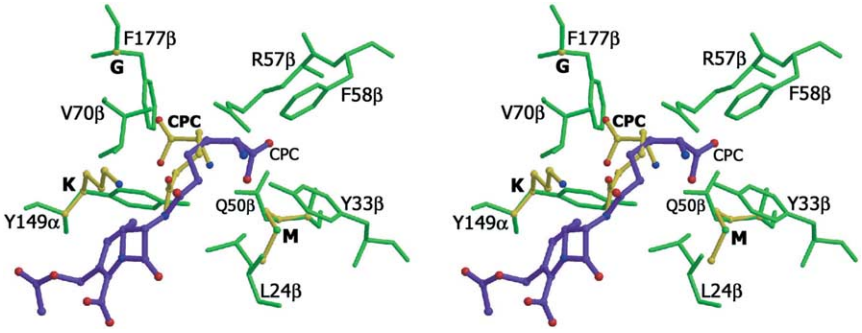

Fig. 2. A model of the CPC-bound triple mutant (Q50βM/Y149αK/F177βG). The D-α-aminoadipyl moiety of CPC in the wild-type is shown in purple and normal letters "CPC" and that of CPC in the triple mutant is proposed to move to the space generated by the triple mutations as shown in yellow and bold letters "**CPC**" [13]. The mutated residues of the model in yellow (M50β as **M**, K149α as **K**, and G177β as **G** in bold letters) are overlaid onto the wild-type residues in green at the same position. The mutant residues Q50βM, Y149αK, and F177βG are modeled such that favorable torsion angles for the three residues are chosen from the ROTAMER database of the program O [17].

deacylation activity of CAD–CPC was gradually improved by this cumulative saturation mutagenesis until the third round of mutation. It may, therefore, be proposed that the deacylation activity to CPC would be improved more with additional rounds of mutation in the active-site residues.

Different substrate specificities between CA and PGA may be due to side-chain conformation of active-site residues

The Cα backbone of CA in the active-site was superimposed on that of PGA, within 1.4 Å (Fig. 3) [11], which implies that the active-site conformations are nearly identical between CAD and PGA. The side-chain conformations of the active-site residues in PGA might differentiate its substrate specificity from that of CAD with varying side-chain conformations. PGA takes the phenyl acetyl group (bulky aromatic chain) as the side-chain moiety of a substrate, penicillin G; whereas, CA takes the glutaryl group (linear aliphatic chain) as a side-chain of GL-7-ACA. It has been proposed that the two fused β-lactam rings of the substrates (both penicillin G and GL-7-ACA) are not dominating elements for the substrate binding into the active-site [13]. Two side-chain moieties of GL-7-ACA and CPC bind to their side-chain pockets; the conformation of the pocket is suited to accommodate the optimal binding interaction with the cognate side-chains of their substrates.

Apparently, different substrate specificities in CA and PGA might be due to the side-chain conformation of the active-site residues, which prompted us to carry out saturation mutagenesis for the side-chain conformation in order to change the substrate specificity of CAD. As a result, the proposition turned out to be proper until the third round of mutagenesis by increasing the deacylation activity to CPC. Furthermore, it seems likely that the deacylation activity of CAD may be converted to that of PGA by mutating the side-chain conformation of the active-site residues of CA in accordance with those of PGA.

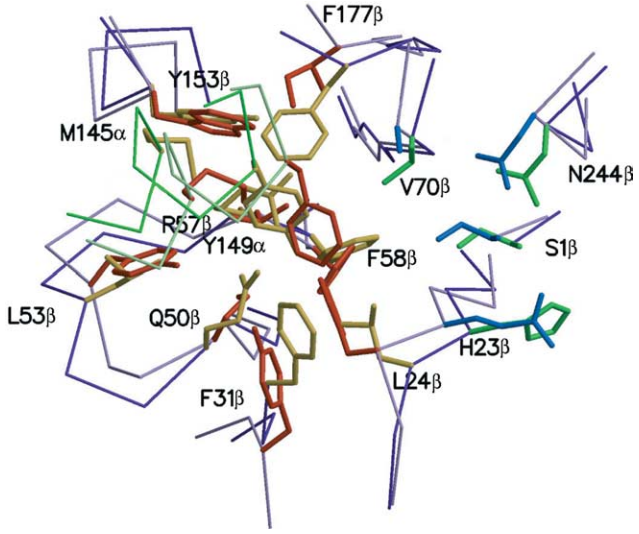

Fig. 3. Active-site superposition between CAD and PGA [1,11]. The Cα atoms of the 61 residues located in close proximity of active-site clefts were used for the superposition. The 14 residues forming the active-site pocket for chemical catalysis and side chain binding are shown. The Cα traces of α- and β-subunits for CAD are colored in green and purple, respectively, and the α- and β-subunits of PGA are shown in light-green and light-purple. The residues involved in chemical catalysis of CAD and PGA are colored in green and blue, respectively, and the ones for the side chain binding pocket of CAD and PGA in yellow and orange. Arg57β of CAD, corresponding to Val56β of PGA, may be most critically involved in altering substrate specificities between two enzymes. Ser1β, His23β, Val70β, Asn244β, Met145α, Tyr149α, Leu24β, Phe31β, Gln50β, Leu53β, Arg57β, Phe58β, Tyr153β, and Phe177β of CAD are structurally aligned to Ser1β, Gln23β, Ala69β, Asn241β, Met142α, Phe146α, Phe24β, Tyr31β, Pro49β, Tyr52β, Val56β, Phe57β, Trp154β, and Ile177β of PGA, respectively.

Modeling of the triple mutant (Q50βM/Y149αK/F177βG) with highest deacylation activity

The triple mutant, Q50βM/Y149αK/F177βG, showed about an 8-fold higher deacylation activity in regard to CPC than the wild-type did (Tables 2–4). Whether the

Table 4
The effect of a third mutation for the double mutant Q50βM/Y149αK on deacylation activity with regard to CPC

Residue for mutation[a]	Mutated to	CPC activity[b] (%)
Phe177β	Pro	301
	Gly	**787**
	Ser	456
Tyr33β	Ser	**568**
	Asn	460
	Thr	424
Met145α	Ala	335
	Pro	442
	Leu	**704**
	Thr	433
Wild-type	Wild	100

[a] Template for mutation is Q50βM/Y149αK.
[b] Legend is the same as in Table 2.

improvement of the deacylation activity is because of the favorable accommodation of the D-α-aminoadipyl moiety of CPC into the newly generated side-chain pocket was carefully examined by modeling the triple mutant enzyme into the active-site (Fig. 2).

The model was built to accommodate the conformation of the D-α-aminoadipyl moiety of CPC more favorably than the wild-type so that it could explain the improvement of deacylation activity for the triple mutant Q50βM/Y149αK/F177βG. In practice, the modeling was to generate room to accommodate the D-α-aminoadipyl moiety of CPC by changing only the side-chains of the target residues with the same main-chain backbone (Fig. 2). Changing the side-chains was carried out by virtual mutagenesis on each residue. The torsion angle of the mutated side-chain was optimized for the side-chain to fit into the newly generated pocket (Fig. 2), so as to favorably accommodate the D-α-aminoadipyl moiety of CPC. When the torsion angles of the mutated side-chains were optimized for the newly generated pocket, those of the D-α-aminoadipyl moiety of CPC were also adjusted to favorably contact the side-chains of the mutated residues. Modeling was carried out by the O program [17]. The favorable torsions for the side-chain conformations were selected from the ROTAMER database. The torsional adjustments were accomplished by the option TORSION in the O program [17].

Once Q50β is mutated to Met, two hydrogen bonds of Q50β (positioning R57β and Y149α to the right orientations) are broken (Fig. 1A, Fig. 2). When Y149α is mutated to Lys, then the active-site residues that bind to the side-chain of the substrate, GL-7-ACA, can move with more freedom to different torsion angles (Fig. 1A, Fig. 2). In addition, the mutation of F177β to Gly would provide empty space where the D-α-aminoadipyl moiety of CPC could move by torsional movement (Fig. 2). As a result, the loosened interactions and lesser side-chain volumes of the mutated residues (Q50βM, Y149αK, and F177βG) would enable the D-α-aminoadipyl moiety of CPC to move into the newly generated side-chain pocket as proposed (Fig. 2).

Intramolecular cleavage may hamper screening of the mutants with higher deacylation activity

The Y33β and F58β mutations produced nine mutants, while the Y149α mutations only produced two mutants, even though we picked up the same number of colonies (40 colonies) from the saturation mutagenesis (Table 3). One possible explanation for the different number of mutants may be that the Y149α mutation can only tolerate a limited number of amino acids in the position, therefore, some amino acids may not be tolerable for proper folding. On the other hand, unfavorable amino acids in the position may prohibit the precursor form of mutant CAs from proceeding through the intramolecular cleavage.

The latter case was previously observed in some portion of the CA mutants where the intramolecular auto-catalytic cleavage did not occur [14,18], which resulted in mutant precursor CAs with no deacylation activity. Therefore, it would be possible that some mutants, even if they would be destined to carry a higher deacylation activity to CPC, could not be processed to mature CAs because of not completing the step of intramolecular cleavage. In order to screen all of the possible mutants in protein engineering, saturation mutagenesis would be carried out with the DNA of mature CA rather than the DNA of precursor CA.

Perspective on obtaining an industrially applicable enzyme

CAD is a class I CA, like CA from *Pseudomonas* sp. 130 (P130) (Table 1). Thirteen active-site residues are identical to these two CAs [11]. In addition, their amino acid sequences are nearly identical, except for 11 out of the 598 residues (91 residues from both CAD and P130 are not included in this sequence comparison, because the 91 residues of P130 may need to be corrected in the amino acid sequence [11]). The nearly identical class I CAs, P130 and CAD, showed about 2% of the deacylation activity to CPC, compared to GL-7-ACA (Table 1). Our mutational study increased the deacylation activity to CPC by 790% and thus, the deacylation activity to CPC for the triple mutant Q50βM/Y149αK/F177βG increased to about 16% (compared to that of GL-7-ACA of the wild-type). This is then a significant accomplishment in improving the deacylation activity to CPC in CA.

Based on the notion of changing the side-chain conformation of active-site residues in CAs, another study

of saturation mutagenesis has been carried out for a different CA. Its deacylation activity to CPC could be increased to over 50% compared to that of GL-7-ACA in the wild-type. The conversion rate of 50% was evaluated as economically applicable for the industrial production of 7-ACA by using a single CA (Y. Kim et al., a manuscript will be published elsewhere).

Our current study is an efficient method for improving the deacylation activity to CPC by employing the structure-based repetitive saturation mutagenesis for the active-site residues of CA. In the near future, mutant CAs, obtained from our experiment, should help to start up industrial application of the single enzyme process for 7-ACA production [5,18].

Acknowledgments

This study was supported by a grant of the Korea Health 21 R&D Project, Ministry of Health & Welfare, Republic of Korea (01-PJ1-PG3-20900-0009), to Y. Kim. We thank Drs. H.S. Lee, K.H. Kim, and S.S. Cha for assistance in the 6B MX beamline of the Pohang Accelerator Laboratory.

References

[1] H.J. Duggleby, S.P. Tolley, C.P. Hill, E.J. Dodson, G. Dodson, P.C. Moody, Penicillin acylase has a single-amino-acid catalytic centre, Nature 373 (1995) 264–268.

[2] F. Huber, R. Chauvette, B. Jackson, Preparative methods for 7-aminocephalosporanic acid and 6-aminopenicillanic acid, in: E. Flynn (Ed.), Chemistry and Biology, Academic press, New York, 1972, pp. 27–48.

[3] I. Aramori, M. Fukagawa, M. Tsumura, M. Iwani, H. Ono, Y. Ishitani, H. Kojo, M. Kohsaka, Y. Ueda, H. Imanaka, Comparative characterization of new glutaryl 7-ACA and Sephalosporin C acylase, J. Ferment. Bioeng. 73 (1992) 185–192.

[4] A. Matsuda, K. Matsuyama, K. Yamamoto, S. Ichikawa, K. Komatsu, Cloning and characterization of the genes for two distinct cephalosporin acylases from a *Pseudomonas* strain, J. Bacteriol. 169 (1987) 5815–5820.

[5] W. Tischer, U. Giesecke, G. Lang, A. Roder, F. Wedekind, Biocatalytic 7-aminocephalosporanic acid production, Ann. N.Y. Acad. Sci. 672 (1992) 502–509.

[6] Y. Ishii, Y. Saito, T. Fujimura, H. Sasaki, Y. Noguchi, H. Yamada, M. Niwa, K. Shimomura, High-level production, chemical modification and site-directed mutagenesis of a cephalosporin C acylase from Pseudomonas strain N176, Eur. J. Biochem. 230 (1995) 773–778.

[7] Y. Saito, T. Fujimura, Y. Ishii, Y. Noguchi, T. Miura, M. Niwa, K. Shimomura, Oxidative modification of a cephalosporin C acylase from Pseudomonas strain N176 and site-directed mutagenesis of the gene, Appl. Environ. Microbiol. 62 (1996) 2919–2925.

[8] Y. Li, J. Chen, W. Jiang, X. Mao, G. Zhao, E. Wang, In vivo post-translational processing and subunit reconstitution of cephalosporin acylase from Pseudomonas sp. 130, Eur. J. Biochem. 262 (1999) 713–719.

[9] Y.S. Lee, S.S. Park, Two-step autocatalytic processing of the glutaryl 7-aminocephalosporanic acid acylase from *Pseudomonas* sp. strain GK16, J. Bacteriol. 180 (1998) 4576–4582.

[10] Y.S. Lee, H.W. Kim, S.S. Park, The role of α-amino group of the N-terminal serine of β subunit for enzyme catalysis and autoproteolytic activation of glutaryl 7-aminocephalosporanic acid acylase, J. Biol. Chem. 275 (2000) 39200–39206.

[11] Y. Kim, K.H. Yoon, Y. Khang, S. Turley, W.J.G. Hol, The 2.0 Å crystal structure of cephalosporin acylase, Structure 8 (2000) 1059–1068.

[12] D.W. Kim, S.M. Kang, K.H. Yoon, Isolation of novel *Pseudomonas diminuta* KAC-1 strain producing glutaryl 7-aminocephalosporanic acid acylase, J. Microbiol. 37 (1999) 200–205.

[13] Y. Kim, G.J.W. Hol, Structure of cephalosporin acylase in complex with glutaryl-7-aminocephalosporanic acid and glutarate: insight into the basis of its substrate specificity, Chem. Biol. 8 (2001) 1253–1264.

[14] S. Kim, Y. Kim, Active site residues of cephalosporin acylase are critical not only for enzymatic catalysis but also for post-translational modification, J. Biol. Chem. 276 (2001) 48376–48381.

[15] J. Sambrook, E.F. Fritsch, T. Maniatis, Molecular Cloning: A Laboratory Manual, second ed., Cold Spring Harbor Laboratory, Cold Spring Harbor, New York, 1989.

[16] Y.S. Lee, H.C. Yang, S.S. Park, Cloning and characterization of GL-7-ACA acylase gene from *Pseudomonas* sp. GK16, J. Microbiol. Biotechnol. 6 (1996) 375–380.

[17] T.A. Jones, J.Y. Zou, S.W. Cowan, M. Kjeldgaard, Improved methods for binding protein models in electron density maps and the location of errors in these models, Acta Crystallogr. A 47 (1991) 110–119.

[18] Y. Kim, S. Kim, N.T. Earnest, G.J.H. Hol, Precursor structure of cephalosporin acylase: insights into autoproteolytic activation in a new N-terminal hydrolase family, J. Biol. Chem. 277 (2002) 2823–2829.

[19] A.C. Wallace, R.A. Laskowski, J.M. Thornton, LIGPLOT: a program to generate schematic diagrams of protein–ligand interactions, Protein Eng. 8 (1995) 127–134.